

Supplementary Information for the paper

Coupling between internal dynamics and rotational diffusion in the presence of exchange between discrete molecular conformations

by

Yaroslav Ryabov, G. Marius Clore,† and Charles D. Schwieters**

*Division of Computational Bioscience, Building 12A, Center for Information Technology, National Institutes of Health, Bethesda, Maryland 20892-5624, and †Laboratory of Chemical Physics, Building 5, National Institutes of Diabetes and Digestive and Kidney Diseases, National Institutes of Health, Bethesda, Maryland 20892-0520

Here we discuss two particular types of symmetry for rotational diffusion tensors \mathfrak{D}^ε for the case of conformational exchange between two states. In addition we provide illustrative numerical Monte Carlo simulations of $C(t)$, and an illustrative calculation of the ratio of NMR relaxation rates for a protein undergoing a hypothetical transition between two states.

Axially symmetric diffusion tensors

In this section we discuss the situation when a solute molecule adopts only two discrete conformation states – A and B . We assume that in both of these conformations the overall rotational diffusion tensors \mathfrak{D}^A and \mathfrak{D}^B , represented by 3×3 matrices, are axially symmetric with $\mathfrak{D}_z^A \neq \mathfrak{D}_x^A = \mathfrak{D}_y^B$, $\mathfrak{D}_z^B \neq \mathfrak{D}_x^B = \mathfrak{D}_y^A$, where $\mathfrak{D}_x^\varepsilon$, $\mathfrak{D}_y^\varepsilon$ and $\mathfrak{D}_z^\varepsilon$ denote three eigenvalues. Further, we explicitly denote two eigenvalues $\mathfrak{D}_\parallel^\varepsilon \equiv \mathfrak{D}_z^\varepsilon$ and $\mathfrak{D}_\perp^\varepsilon \equiv \mathfrak{D}_x^\varepsilon = \mathfrak{D}_y^\varepsilon$ corresponding to two vectors of the diffusion tensor principal axis frame which are parallel and perpendicular to its axis of symmetry.

It is well known (1) that for the case of an axially symmetric diffusion tensor \mathfrak{D}^ε , the eigenfunctions of the differential operator $\hat{L}^T \mathfrak{D}^\varepsilon \hat{L}$ are the elements of Wigner rotation matrices

$$\hat{L}^T \mathfrak{D}^\varepsilon \hat{L} D_{nm}^l(\Omega_\varepsilon) = \Lambda_m^{\varepsilon,l} D_{nm}^l(\Omega_\varepsilon) \quad [\text{S1}]$$

where Ω_ε specifies the orientation of the principal axis frame of the diffusion tensor matrix \mathfrak{D}^ε . Here we consider the case $l = 2$ (appropriate for NMR relaxation). Then the five eigenvalues of Eq. [S1] are given as

$$\Lambda_m^\varepsilon = 6\mathfrak{D}_\perp^\varepsilon + m^2(\mathfrak{D}_\parallel^\varepsilon - \mathfrak{D}_\perp^\varepsilon) \quad [\text{S2}]$$

According to their definitions, in the axially symmetric case the unitary transformations \mathbf{U}^{AB} and $\mathbf{U}^{BA} = (\mathbf{U}^{AB})^\dagger$ specify transitions between two sets of $D_{nm}^2(\Omega_A)$ and $D_{nm}^2(\Omega_B)$. However, due to the

axial symmetry of both \mathfrak{D}^A and \mathfrak{D}^B , in this case the choice for Ω_A and Ω_B is not unique: it is only necessary that the z axes of the principal axis frames of tensors \mathfrak{D}^A and \mathfrak{D}^B are oriented along the axes of symmetry of \mathfrak{D}^A and \mathfrak{D}^B while the orientations of x and y are not fixed. We use this freedom in the definitions of Ω_A and Ω_B to define transformations \mathbf{U}^{AB} and \mathbf{U}^{BA} in the most convenient way. Thus, we define the principal axis frames of tensors \mathfrak{D}^A and \mathfrak{D}^B in such a way that their y-axes have the same orientation. This is always possible for any mutual orientation of axially symmetric tensors \mathfrak{D}^A and \mathfrak{D}^B . In this case the transition between the sets of $D_{nm}^2(\Omega_A)$ and $D_{nm}^2(\Omega_B)$ can be encoded by a single Euler angle β_{AB} defining the tilt between axes of symmetry of \mathfrak{D}^B and \mathfrak{D}^A . Then the unitary transformation \mathbf{U}^{AB} is

$$[\mathbf{U}^{AB}]_{nm} = [(\mathbf{U}^{BA})^\dagger]_{nm} = d_{nm}^2(\beta_{AB}) \quad [\text{S3}]$$

where $d_{nm}^2(\beta)$ (see supplementary **Table S1**) are the elements of the reduced Wigner rotation matrix which are used in definition (2) of the full $D_{nm}^l(\Omega)$, where Ω is specified in terms of Euler angles $\{\alpha, \beta, \gamma\}$, as

$$D_{nm}^l(\Omega) = e^{-in\alpha} d_{nm}^l(\beta) e^{-im\gamma} \quad [\text{S4}]$$

For the case of axially symmetric \mathfrak{D}^A and \mathfrak{D}^B the eigenfunctions of operators $\hat{L}^T \mathfrak{D}^A \hat{L}$ and $\hat{L}^T \mathfrak{D}^B \hat{L}$ are Wigner rotation matrices $D_{nm}^2(\Omega_A)$ and $D_{nm}^2(\Omega_B)$. In this case the unitary transformations \mathbf{U}^A and \mathbf{U}^B are specified only by three dimensional rotations Ω_{AM} and Ω_{BM} . Then,

$$\mathbf{Y}_2^T(\Omega_{MI}^\varepsilon) \mathbf{U}^\varepsilon = \sqrt{\frac{5}{4\pi}} \sum_{k=-2}^2 D_{nk}^{2*}(\Omega_{\varepsilon M}) D_{k0}^{2*}(\Omega_{MI}^\varepsilon) = \mathbf{Y}_2^T(\Omega_{\varepsilon I}) \quad [\text{S5}]$$

for $\varepsilon = A, B$ and where $\Omega_{\varepsilon I}$ specifies the orientation of the vector of interest in conformation ε with respect to principal axis frame of \mathfrak{D}^ε .

Anisotropic diffusion tensors

If diffusion tensors \mathfrak{D}^A and \mathfrak{D}^B are not axially symmetric, the eigenfunctions of the differential operators $\hat{L}^T \mathfrak{D}^\varepsilon \hat{L}$ no longer coincide with the Wigner rotation matrices (1). However, the eigenfunctions of those operators can be represented using a basis of Wigner rotation matrices as

$$\psi_{nm}^{\varepsilon, l}(\Omega_\varepsilon) = \sum_{k=-l}^l D_{nk}^l(\Omega_\varepsilon) A_{km}^{\varepsilon, l} \quad [\text{S6}]$$

with the elements of the transformation matrix A_{nk}^l given for $l = 2$ explicitly as

$$\mathbf{A}^\varepsilon = \begin{pmatrix} -\frac{1}{\sqrt{2}} & 0 & 0 & 0 & \frac{1}{\sqrt{2}} \\ 0 & -\frac{1}{\sqrt{2}} & 0 & \frac{1}{\sqrt{2}} & 0 \\ -\frac{u^\varepsilon}{N^\varepsilon\sqrt{2}} & 0 & \frac{w^\varepsilon}{N^\varepsilon} & 0 & -\frac{u^\varepsilon}{N^\varepsilon\sqrt{2}} \\ 0 & \frac{1}{\sqrt{2}} & 0 & \frac{1}{\sqrt{2}} & 0 \\ \frac{w^\varepsilon}{N^\varepsilon\sqrt{2}} & 0 & \frac{u^\varepsilon}{N^\varepsilon} & 0 & \frac{w^\varepsilon}{N^\varepsilon\sqrt{2}} \end{pmatrix} \quad [\text{S7}]$$

where we drop the index l in the definitions for $\mathbf{A}^\varepsilon \equiv \mathbf{A}^{\varepsilon,2}$. The eigenvalues of $\hat{L}^T \mathfrak{D}^\varepsilon \hat{L}$ for a fully anisotropic \mathfrak{D}^ε are (1)

$$\begin{aligned} \Lambda_{-2}^\varepsilon &= 3(\mathfrak{D}_z^\varepsilon + \mathfrak{D}_s^\varepsilon) \\ \Lambda_{-1}^\varepsilon &= 3(\mathfrak{D}_y^\varepsilon + \mathfrak{D}_s^\varepsilon) \\ \Lambda_0^\varepsilon &= 6\mathfrak{D}_s^\varepsilon - 2\Delta^\varepsilon \\ \Lambda_1^\varepsilon &= 3(\mathfrak{D}_x^\varepsilon + \mathfrak{D}_s^\varepsilon) \\ \Lambda_2^\varepsilon &= 6\mathfrak{D}_s^\varepsilon + 2\Delta^\varepsilon \end{aligned} \quad [\text{S8}]$$

with, $\Delta^\varepsilon = \sqrt{(\mathfrak{D}_x^\varepsilon - \mathfrak{D}_y^\varepsilon)^2 + (\mathfrak{D}_z^\varepsilon - \mathfrak{D}_x^\varepsilon)(\mathfrak{D}_z^\varepsilon - \mathfrak{D}_y^\varepsilon)}$, $w^\varepsilon = 2\mathfrak{D}_z^\varepsilon - \mathfrak{D}_x^\varepsilon - \mathfrak{D}_y^\varepsilon + 2\Delta^\varepsilon$, $N^\varepsilon = 2\sqrt{|\Delta^\varepsilon w^\varepsilon|}$, $u^\varepsilon = \sqrt{3}(\mathfrak{D}_x^\varepsilon - \mathfrak{D}_y^\varepsilon)$, and $\mathfrak{D}_s^\varepsilon = (\mathfrak{D}_x^\varepsilon + \mathfrak{D}_y^\varepsilon + \mathfrak{D}_z^\varepsilon)/3$, except for the very specific case of axially symmetric oblate tensor with $\mathfrak{D}_z^\varepsilon < \mathfrak{D}_x^\varepsilon = \mathfrak{D}_y^\varepsilon$ when the expressions for Δ^ε and w^ε should change their signs: $\Delta^\varepsilon = -\sqrt{(\mathfrak{D}_x^\varepsilon - \mathfrak{D}_y^\varepsilon)^2 + (\mathfrak{D}_z^\varepsilon - \mathfrak{D}_x^\varepsilon)(\mathfrak{D}_z^\varepsilon - \mathfrak{D}_y^\varepsilon)}$ and $w^\varepsilon = -2\mathfrak{D}_z^\varepsilon + \mathfrak{D}_x^\varepsilon + \mathfrak{D}_y^\varepsilon - 2\Delta^\varepsilon$.

It is instructive to discuss the limiting transition of Eqs. [S6], [S7] and [S8] to the axially symmetric case when $\mathfrak{D}_x^\varepsilon = \mathfrak{D}_y^\varepsilon$. It can be verified that in this limit Eqs. [S8] reproduce the eigenvalues of the axially symmetric top in Eq. [S2]. However, is also easy to see that in this case $w^\varepsilon/N^\varepsilon = 1$, $u^\varepsilon/N^\varepsilon = 0$ and the eigenfunctions defined by Eq. [S6] do not reduce to the definitions of the eigenfunctions of the axially symmetric case [S1]. This discrepancy is due to the degeneracy of the eigenvalues, $\Lambda_m^\varepsilon = \Lambda_{-m}^\varepsilon$, of the $\hat{L}^T \mathfrak{D}^\varepsilon \hat{L}$ operators in the axially symmetric case. However, in the axially symmetric case, instead of $D_{n,m}^2(\Omega_\varepsilon)$ and $D_{n,-m}^2(\Omega_\varepsilon)$ one can use two orthogonal normalized linear combinations of these eigenfunctions, such that $\Psi_{n,m}^\varepsilon(\Omega_\varepsilon) = (D_{n,m}^2(\Omega_\varepsilon) + D_{n,-m}^2(\Omega_\varepsilon))/\sqrt{2}$ for $m > 0$ and $\Psi_{n,m}^\varepsilon(\Omega_\varepsilon) = (D_{n,m}^2(\Omega_\varepsilon) - D_{n,-m}^2(\Omega_\varepsilon))/\sqrt{2}$ for $m < 0$.

In contrast to the axially symmetric case discussed above, for fully anisotropic diffusion tensors there is no freedom in defining the orientations of the principal axis frames. In addition, since the eigenfunctions of differential operators $\hat{L}^T \mathfrak{D}^\varepsilon \hat{L}$ are no longer Wigner rotation matrices, the transformation matrix \mathbf{U}^{AB} is expressed as

$$\mathbf{U}^{AB} = (\mathbf{U}^{BA})^\dagger = \mathbf{A}^A \mathbf{D}(\Omega_{AB}) \mathbf{A}^{B\dagger} \quad [\text{S9}]$$

where matrix $[\mathbf{D}(\Omega_{AB})]_{nm} = D_{nm}^2(\Omega_{AB})$ and Ω_{AB} specifies the rotational transformation from the principal axis frame of \mathfrak{D}^B to the principal axis frame of \mathfrak{D}^A . Similarly, in the case of anisotropic diffusion tensors the product $\mathbf{Y}_2^T(\Omega_{MI}^\varepsilon) \mathbf{U}^\varepsilon$ not only accounts for the orientation of the vector of interest but is also dependent on the parameters of transformation \mathbf{A}^ε as follows

$$\mathbf{Y}_2^T(\Omega_{MI}^\varepsilon) \mathbf{U}^\varepsilon = \mathbf{Y}_2^T(\Omega_{\varepsilon I}) \mathbf{A}^{\varepsilon\dagger} \quad [\text{S10}]$$

Comparison with simulation results in the time domain

The closed form solution in the frequency domain for the Laplace transformed correlation function $\tilde{C}(\sigma)$ is represented by the Eqs. [22] and [23] of the main text. To convert this solution into the time domain one needs to obtain the time domain representation of the rate matrices $\mathbf{R}^{\varepsilon\eta}(\sigma)$ using the inverse Laplace transform \mathcal{L}^{-1} (3) which is represented by the Bromwich integral

$$\mathcal{L}^{-1}\{\mathbf{R}^{\varepsilon\eta}(\sigma)\}(t) \equiv \frac{1}{2\pi i} \lim_{\omega \rightarrow +\infty} \int_{\gamma-i\omega}^{\gamma+i\omega} \mathbf{R}^{\varepsilon\eta}(\sigma) e^{\sigma t} d\sigma \quad [\text{S11}]$$

According to the Cauchy residue theorem (4), a closed loop integral, like the Bromwich integral [S11], is equal to the sum of the residues of the function of interest

$$\mathcal{L}^{-1}\{\mathbf{R}^{\varepsilon\eta}(\sigma)\}(t) = \sum_{r_k} \lim_{\sigma \rightarrow r_k} (\sigma - r_k) \mathbf{R}^{\varepsilon\eta}(\sigma) e^{\sigma t} \quad [\text{S12}]$$

where r_k are all the poles of $\mathbf{R}^{\varepsilon\eta}(\sigma)$ on the complex manifold. It is clear from Eq. [23] that these poles originate from the roots of the matrix denominators of rate matrices $\mathbf{R}^{\varepsilon\eta}(\sigma)$ *i.e.* r_k are given by the algebraic equation

$$\det(\mathbf{Q}^A \mathbf{U}^{AB} \mathbf{Q}^B - k_{AB} k_{BA} \mathbf{U}^{AB}) = \det(\mathbf{Q}^B \mathbf{U}^{BA} \mathbf{Q}^A - k_{AB} k_{BA} \mathbf{U}^{BA}) = 0 \quad [\text{S13}]$$

Finding these roots in closed form is not possible due to the high dimensionality of the problem and the Abel-Ruffini impossibility theorem (5). However, it is always possible to obtain these roots by numerically solving Eq. [S13] for any particular set of numeric parameters of the problem: *i.e.* transition rates k_{AB} and k_{BA} , two sets of eigenvalues $\{\mathfrak{D}_x^A, \mathfrak{D}_y^A, \mathfrak{D}_z^A\}$ and $\{\mathfrak{D}_x^B, \mathfrak{D}_y^B, \mathfrak{D}_z^B\}$ of diffusion tensors \mathfrak{D}^A and \mathfrak{D}^B , and the parameters of Ω_{AB} which specify the rotational transformation between the principal axis frames of \mathfrak{D}^B and \mathfrak{D}^A . Note that the roots of Eq. [S13], and therefore, the time domain representation of $\mathbf{R}^{\varepsilon\eta}(\sigma)$ depend only on these parameters, while the correlation function $C(t)$ is also dependent on

the orientation of the vector of interest: that is on the two sets of Euler angles Ω_{AI} and Ω_{BI} which specify the orientation of this vector in the two conformational states with respect to the principal axis frame of the diffusion tensor of the appropriate conformation.

Substituting the time dependent $\mathcal{L}^{-1}\{\mathbf{R}^{\varepsilon\eta}(\sigma)\}(t)$ from [S12] into Eq. [22] of the main text, instead of the frequency dependent $\mathbf{R}^{\varepsilon\eta}(\sigma)$, one obtains a numerical representation for $C(t)$. To verify the correctness of our solutions we compared the time domain numerical representation of $C(t)$ derived from Eqs. [22], [23], [S12], and [S13] with the results of Monte Carlo simulations.

For simulations of $C(t)$ we used the following approach. Initially we defined two sets of three mutually perpendicular unit vectors representing the orientations of two principal axis frames of molecular diffusion tensors in two conformations, A and B. In addition to these six unit vectors we also define two other unit vectors representing orientations of the vectors of interest in these conformations. Choosing the orientations of those eight unit vectors is equivalent to defining Ω_{AB} , Ω_{AI} and Ω_{BI} . We also chose values of transition rates k_{AB} and k_{BA} and derived from them equilibrium occupation probabilities $P_{eq}(A) = k_{BA}/(k_{AB}+k_{BA})$ and $P_{eq}(B) = k_{AB}/(k_{AB}+k_{BA})$. We then obtain the probability of being in the initial conformation after unit time interval, Δt , as

$$P(\eta, \Delta t | \eta, 0) = P_{eq}(\eta) + P_{eq}(\varepsilon) e^{-(k_{AB}+k_{BA})\Delta t} \quad [\text{S14}]$$

where $\eta \neq \varepsilon$. In the simulations we always assume a unit time step $\Delta t = 1$. Given a current conformation, orientations of the vectors of the principal axis frame of this conformation, and values of the conformation-specific rotational diffusion coefficients $\{\mathcal{D}_x^\varepsilon, \mathcal{D}_y^\varepsilon, \mathcal{D}_z^\varepsilon\}$, one can always explicitly calculate a spatial transformation matrix which specifies a random ‘‘infinitesimal’’ diffusion rotation appropriate for the current molecular conformation.

Thus, the Monte Carlo simulation routine runs as follows. For every Monte Carlo trajectory we choose a random initial conformation state using equilibrium occupation probabilities $P_{eq}(A)$ and $P_{eq}(B)$. Then, we calculate the infinitesimal spatial rotation matrix using the parameters of the current conformation state. We apply the rotational transformation encoded by this matrix to all unit vectors and update their orientations making certain that base vectors remain orthonormal and the vectors which represent the vectors of interest remain of unit length. We record the orientation of the unit vector relevant to the current conformation state. Then, using values of $P(\eta, \Delta t | \eta, 0)$ we choose randomly between the two alternatives: to stay in the current conformation or to change the conformation. After making this decision we close the simulation loop.

We calculate $N_{tr} = 10^4$ different Monte Carlo trajectories where every trajectory consists of $N_{st} = 1.5 \times 10^6$ simulation time steps. For each simulated trajectory we calculate the orientation correlation function of the vector of interest

$$C(z) = \frac{1}{N_{st} - z} \sum_{k=0}^{N_{st}-z} P_2[\mathbf{n}(k) \cdot \mathbf{n}(k+z)] \quad [\text{S15}]$$

where $z = t/\Delta t$ is a dimensionless discrete time variable. As can be seen from Eq. **[S15]** this method for evaluation of $C(z)$ yields different sampling efficacy for different time moments z due to the finite value of N_{st} . Thus, even in the case where the trajectories are relatively long, we limit the calculations of $C(z)$ to the relatively small value of $z_{max} = 10^3$ to maintain less than 0.07% difference in sampling number between $C(0)$ and $C(z_{max})$. Finally, we average $C(z)$ obtained from different Monte Carlo trajectories.

Fig. S1 presents the comparison between $C_{theor}(t)$ calculated using theoretical expressions **[22]**, **[23]**, **[S12]**, **[S13]** and $C_{sim}(t)$ obtained from simulations for the case where in both conformation states the rotational dynamics of the molecule under consideration is described by fully the anisotropic diffusion tensors \mathfrak{D}^A and \mathfrak{D}^B . This figure shows that averaging more than a hundred Monte Carlo trajectories yields simulation results that are virtually indistinguishable from the theoretical $C_{theor}(t)$ curve. More detailed comparison in **Fig. S2** also reveals a clear tendency for the difference $\Delta C(t) = C_{theor}(t) - C_{sim}(t)$ to decrease with increasing number of different Monte Carlo trajectories used for averaging when estimating $C_{sim}(t)$. In **Fig. S3** the variance $Var = \sqrt{\langle(\Delta C(t) - \langle\Delta C(t)\rangle)^2\rangle}$ obeys the theoretical dependency $Var \sim 1/\sqrt{N_{av}}$ where N_{av} is the number of trajectories used for averaging.

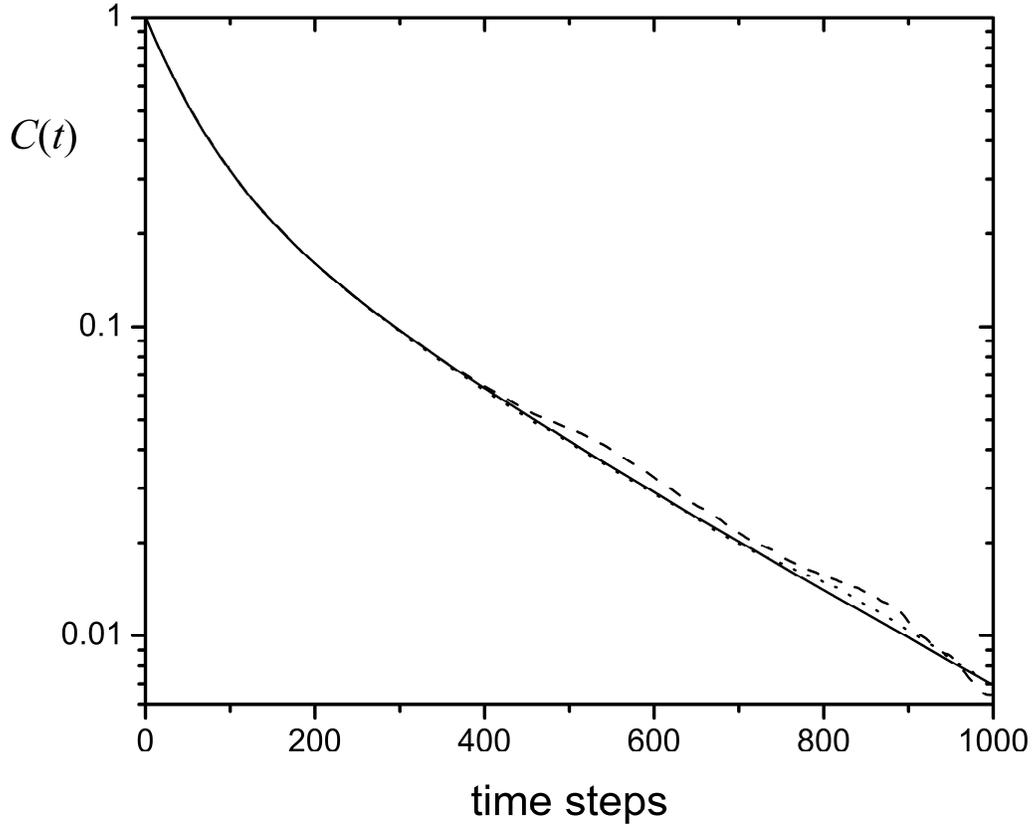


Fig. S1 Comparison between the theoretical time dependency of the orientation correlation function $C_{theor}(t)$, represented by the solid line, and the simulated $C_{sim}(t)$: the dashed line represents a single Monte Carlo trajectory, while the dotted line represents $C_{sim}(t)$ averaged over 10 trajectories. All the calculations were performed for the following set of parameters: $\mathcal{D}_x^A = 3 \times 10^{-4}$, $\mathcal{D}_y^A = 6 \times 10^{-4}$, $\mathcal{D}_z^A = 1 \times 10^{-3}$, $\mathcal{D}_x^B = 2 \times 10^{-4}$, $\mathcal{D}_y^B = 7 \times 10^{-4}$, $\mathcal{D}_z^B = 6 \times 10^{-3}$, $k_{AB} = 7 \times 10^{-3}$, $k_{BA} = 9 \times 10^{-3}$, $\Omega_{AB}: \{\alpha_{AB} = 27, \beta_{AB} = 78, \gamma_{AB} = 17\}$, $\Omega_{AI}: \{\alpha_{AI} = 72, \beta_{AI} = 37\}$, and $\Omega_{BI}: \{\alpha_{BI} = 24, \beta_{BI} = 17\}$ where all the components of the diffusion tensors and transition rates are given per unit time interval Δt , and all the angles are in degrees.

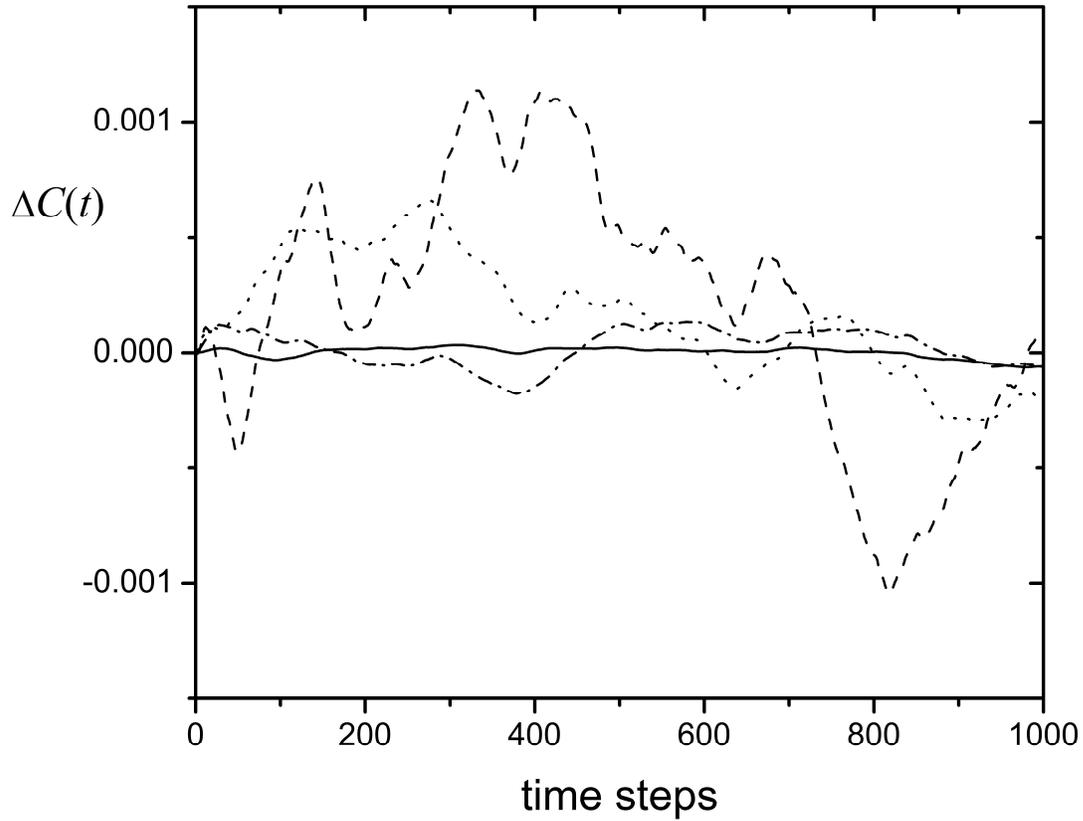


Fig. S2 Difference, $\Delta C(t)$, between theoretical, $C_{theor}(t)$, and simulated, $C_{sim}(t)$, values of the orientation correlation function for different numbers of Monte Carlo trajectories used for $C_{sim}(t)$ averaging: dashed line, 10^1 ; dotted line, 10^2 ; dash-dotted, 10^3 ; and solid line, 10^4 trajectories. All calculations were performed using the set of parameters given in the legend of **Fig. S1**.

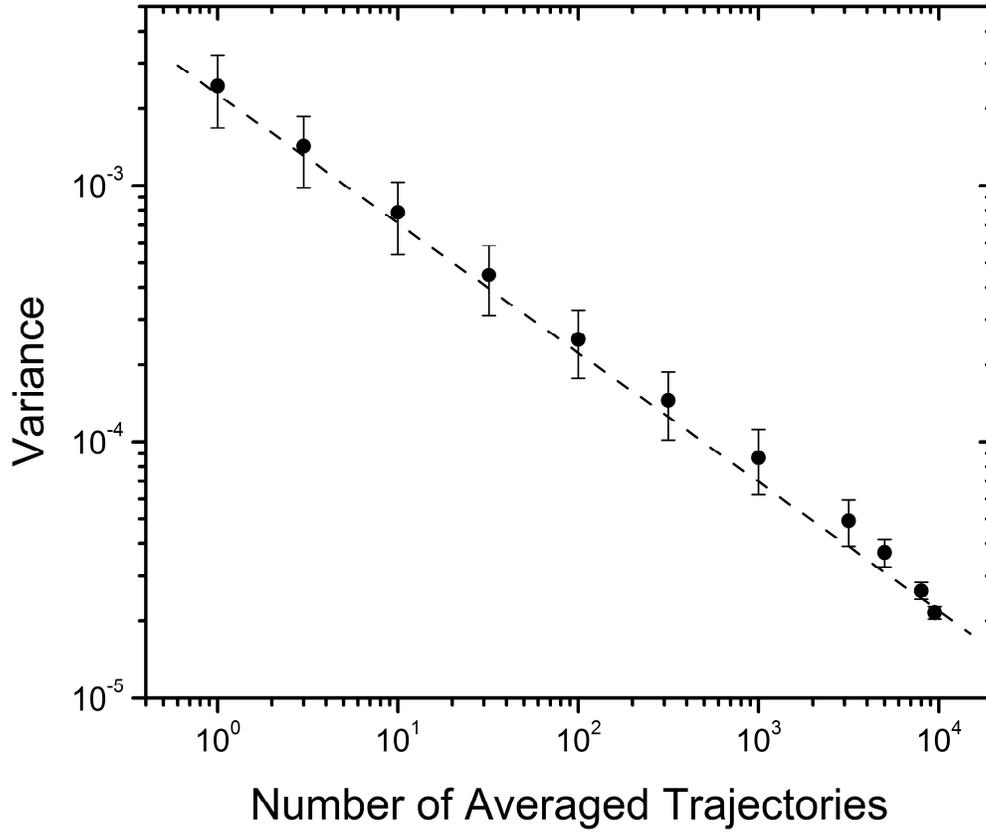


Fig. S3 Dependence of the variance between theoretical $C_{theor}(t)$ and simulated $C_{sim}(t)$ on the number of Monte Carlo trajectories used for $C_{sim}(t)$ averaging. Symbols represent the averaged values of variances calculated for different possibilities for selecting N_{av} trajectories for averaging from the total number N_{tr} of all calculated trajectories. The dashed line represents the theoretical dependence $Var \sim 1/\sqrt{N_{av}}$. All calculations were performed using the set of parameters given in the legend of **Fig. S1**.

Illustrative calculations of NMR relaxation rates

To illustrate the potential impact of the internal dynamics on experimental observables we present here the results of numerical calculations on NMR relaxation data using a hypothetical protein system. We calculate the ratio of R_2 and R_1 , the transverse and longitudinal relaxation rates, respectively. To calculate these rates we use the standard relationships (6) between the spectral density, $J(\omega)$, and relaxation rates. The spectral density was obtained directly from Laplace image $\tilde{C}(\sigma)$ of orientation correlation function defined by Eq. [22] using the relationships between Laplace and Fourier transformations $J(\omega) = Re\{\hat{C}(\omega)\} = Re\{\tilde{C}(\sigma)|_{\sigma=i\omega}\}$.

We calculated NMR relaxation rates for each backbone NH pair in the protein. We assumed no effects of anisotropy of the chemical shielding tensor by assuming a CSA constant equal to zero. We evaluated the relaxation rates at specific spectrometer frequency of 600.141 MHz.

We used the symmetric 128 kDa dimer complex of enzyme I (EI), which is the first component of the bacterial phosphotransferase system of Escherichia Coli, as an example of the system exhibiting large scale conformation exchange between two states (7).

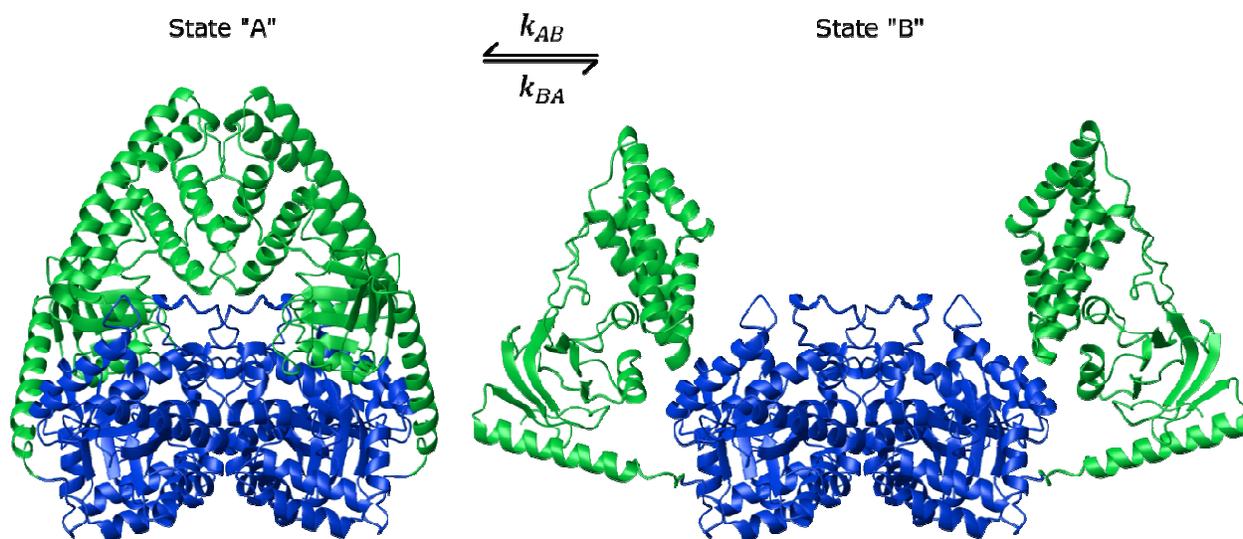


Fig. S4 Two conformation states of EI dimer: N-terminal domains of the dimer are green, C-terminal domains are blue.

We evaluated the components of the rotational diffusion tensors of each conformation using the built-in computational facilities of Xplor-NIH (8) assuming that EI tumbles in water at 300 K and obtained the values

$$\mathcal{D}_x^A = 29.16 \times 10^7 [s^{-1}], \mathcal{D}_y^A = 31.47 \times 10^7 [s^{-1}], \mathcal{D}_z^A = 32.43 \times 10^7 [s^{-1}]$$

$$\mathcal{D}_x^B = 15.71 \times 10^7 [s^{-1}], \mathcal{D}_y^B = 15.82 \times 10^7 [s^{-1}], \mathcal{D}_z^B = 30.99 \times 10^7 [s^{-1}]$$

with the overall rotational correlation time $\tau^A = 53.73$ ns for state A and $\tau^B = 79.99$ ns for state B. The process of conformational exchange between the two conformations depicted above purely hypothetical. For our illustrative purposes we assume the transition rates k_{AB} and k_{BA} are equal $k_{AB} = k_{BA}$ which leads to equal occupation probabilities $P_{eq}(A) = P_{eq}(B) = 1/2$. We conducted

calculations for three regimes: when the rates of conformational exchange are comparable to the scale of overall rotational diffusion $k = k_{AB} = k_{BA} = 155.57 \times 10^7 [s^{-1}]$ and for the situations of fast and slow exchange, $k_{fast} = 10 \times k$ and $k_{slow} = 0.1 \times k$. We also assumed that the conformation transition depicted in Fig. S4 preserves orientation of the PAF of diffusion tensors.

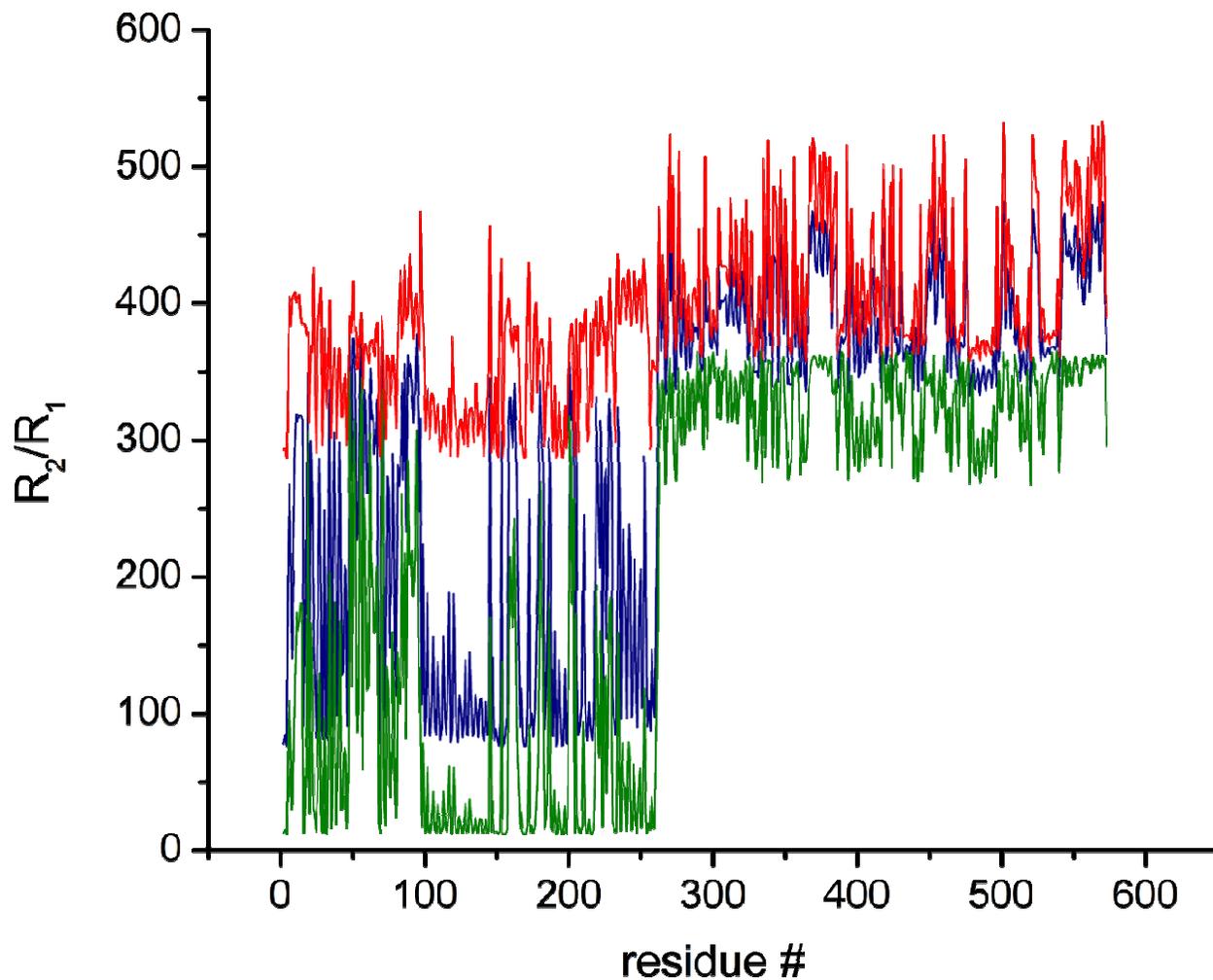


Fig. S5 Simulated ratios of EI relaxation rates R_2/R_1 . The blue curve corresponds to $k = 155.57 \times 10^7 [s^{-1}]$, red line is for the case of slow exchange $k_{slow} = 0.1 \times k$, green line is for the case of fast exchange, $k_{fast} = 10 \times k$. In this figure the N-terminal domain of EI spans residues 1-259 and residues 260-573 comprise the C-terminal domain.

Table S1 Components of the reduced Wigner rotation matrices $d_{n,m}^2(\beta)$

$$d_{2,2}^2(\beta) = \left(\frac{1 + \cos(\beta)}{2}\right)^2$$

$$d_{2,1}^2(\beta) = -\frac{1 + \cos(\beta)}{2} \sin(\beta)$$

$$d_{2,0}^2(\beta) = \frac{\sqrt{6}}{4} \sin^2(\beta)$$

$$d_{2,-1}^2(\beta) = -\frac{1 - \cos(\beta)}{2} \sin(\beta)$$

$$d_{2,-2}^2(\beta) = \left(\frac{1 - \cos(\beta)}{2}\right)^2$$

$$d_{1,1}^2(\beta) = \frac{1 + \cos(\beta)}{2} (2 \cos(\beta) - 1)$$

$$d_{1,0}^2(\beta) = -\sqrt{\frac{3}{2}} \sin(\beta) \cos(\beta)$$

$$d_{1,-1}^2(\beta) = \frac{1 - \cos(\beta)}{2} (2 \cos(\beta) + 1)$$

$$d_{0,0}^2(\beta) = \frac{3 \cos^2(\beta) - 1}{2}$$

and the rest of matrix elements can be obtained using the symmetry relationships

$$d_{n,m}^2(\beta) = (-1)^{m-n} d_{n,n}^2(\beta) = d_{-m,-n}^2(\beta)$$

1. Favro LD (1960) Theory of the Rotational Brownian Motion of a Free Rigid Body. *Phys Rev* **119**:53-62.
2. Brink DM, Satchler GR (1968) *Angular momentum* (Clarendon P., Oxford).
3. Abramowitz M, Stegun IA (1964) *Handbook of mathematical functions with formulas, graphs, and mathematical tables* (U.S. Govt. Print. Off., Washington,).
4. Ahlfors LV (1979) *Complex analysis : an introduction to the theory of analytic functions of one complex variable* (McGraw-Hill, New York).
5. Jacobson N (2009) *Basic algebra* (Dover Publications, Mineola, N.Y.).
6. Abragam A (1961) *The principles of nuclear magnetism* (Clarendon Press, Oxford,).
7. Takayama Y, Schwieters CD, Grishaev A, Ghirlando R, & Clore GM (2011) *J Am Chem Soc* **133**, 424-427.
8. Ryabov Y, Suh JY, Grishaev A, Clore GM, & Schwieters CD (2009) *J Am Chem Soc* **131**, 9522-9531.